Measurement Uncertainty in Network Analyzers: Differential Error DE Analysis of Error Models Part 5: Step-by-Step Graphical Construction of Complex DE Regions and Real DE Intervals

N.I. Yannopoulou, P.E. Zimourtopoulos *

Antennas Research Group, Austria

Abstract

This paper demonstrates the way of how the value of any quantity used in Microwaves and RF and defined, either directly or indirectly, by one ore more complex differentiable functions of one or more Vector Network Analyzer VNA measurements, is affected by its ubiquitous Differential Errors DEs, when these DEs are expressed in terms of the manufacturers' data for both the unavoidable uncertainties of the calibration standards and the inescapable inaccuracies of the VNA indications. This is illustrated by a step-by-step graphical construction of the complex DE Regions DERs and their real rectangular and polar DE Intervals DEIs, which the authors introduced and used in all previous parts of this series. As it is geometrically shown, in order to build the composite figure of any complex DER and then of its DEIs only three basic types of simple figures are needed. These figures result by using combinations of appropriate complex transformations, which are well-known from Complex Analysis, that is: translation, scaling (stretching or shrinking), and rotation. A number of selected applications are presented and some useful, general conclusions are drawn.

Keywords

microwave measurements, network analyzer, differential error region, differential error interval, calibration

Introduction

The Differential Error DE analysis of the Error Models commonly used in VNA calibration: (a) in full one-port measurements [1], [2], (b) in full two-port measurements, with either direct or indirect Through connection [3]-[5], and (c) in just a respon-

se calibration [6], were pre-
sented in details in previ-
ously published authors' work.
The Differential Error Re-
gions DERs and their Diffe-
rential Error Intervals DEIs,
were defined and used in or-
der to estimate the uncer-
tainty in measurements, with
a Vector Network Analyzer
VNA, of one-port and two-port
Devices Under Test, DUTs.
Fig. 1 and Fig. 2 show these
well-known one-port and two-
port Error Model respectively.
To simplify notation, just
one symbol was used for each
one of the complex valued
system errors: (a) D, M, R,

L, T and X, in the forward
direction, (b) D', M', R',
L', T' and X', in the reverse
direction, (c) T_{ij}, for the
S-parameters of Through, and
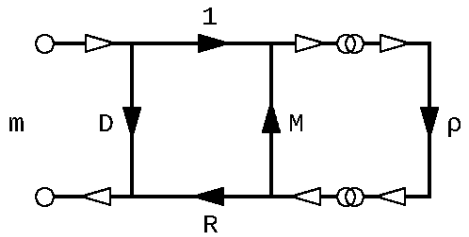(d) m, m_{ij}, for DUT measure-
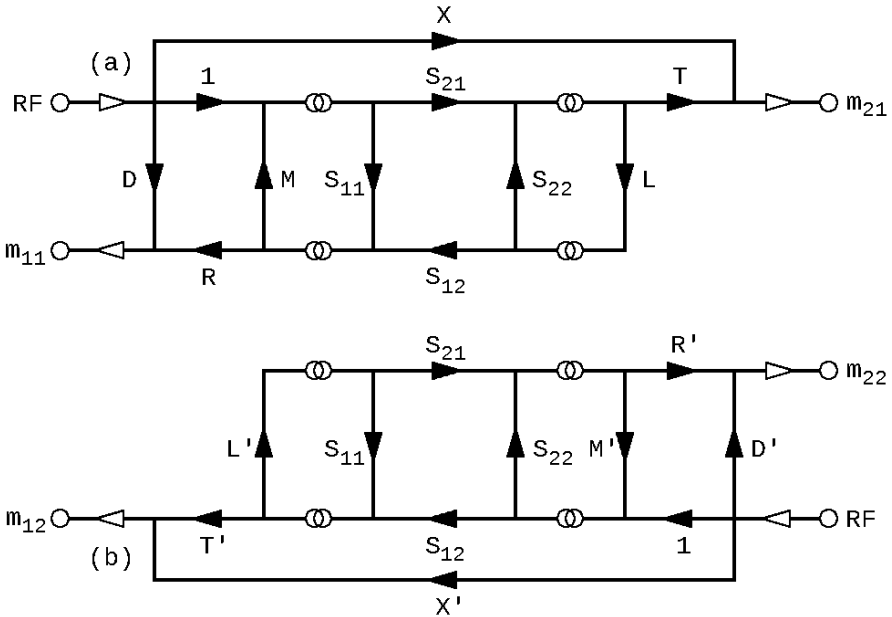ments.

Fig. 1: Full one-port Error
Model

Fig. 2: Full two-port Error Model: forward and reverse

Using the system errors, the measurements, and the data for the uncertainty of standards and inaccuracy of the VNA indications, the Differential Errors can be expressed, in the way developed by the authors, for all commonly used in Microwaves and RF quantities, which are related to VNA measurements, the composite geometric outline of their complex DER can be constructed, and from that the exact real rectangular and polar DEIs can be drawn too.

These DERs are built through addition of the initial simple geometric figures of just three distinguished basic types. A step by step illustrative construction with appropriately selected DERs will facilitate the comprehension of this graphical construction.

The first results in this area were presented by the authors through distance connection to the attendees, both local and distant, of the 30th ANAMET meeting of National Physical Laboratory NPL held in Teddington UK, on 24 October 2008, and since then are available online [7].

Counting Variables

As typical examples, two complex differential errors are given below by (1) and (2).

$$d\rho = [- RdD - (m - D)^2 dM - (m - D)dR + Rdm]/[M(m - D) + R]^2 \tag{1}$$

$$
\begin{aligned}
dS_{12} = \{&T(R'(m_{12} - X')(M - L') - MT'S_{12}[R' + M'(m_{22} - D')])(dm_{11} - dD) \\
&+ R'\{T[R + (m_{11} - D)(M - L')] + RLL'S_{12}(m_{21} - X)\}(dm_{12} - dX') \\
&+ RR'LL'S_{12}(m_{12} - X')(dm_{21} - dX) \\
&- M'T\,T'S_{12}[R + M(m_{11} - D)](dm_{22} - dD') \\
&+ T(m_{11} - D)(R'(m_{12} - X') - T'S_{12}[R' + M'(m_{22} - D')])dM \\
&- T\,T'S_{12}(m_{22} - D')[R + M(m_{11} - D)]dM' \\
&+ (R'(m_{12} - X')[T + LL'S_{12}(m_{21} - X)] - \\
&- T\,T'S_{12}[R' + M'(m_{22} - D')])dR \\
&+ \{(m_{12} - X')(T(m_{11} - D)(M - L') + R[T + LL'S_{12}(m_{21} - X)]) - \\
&- T\,T'S_{12}[R + M(m_{11} - D)]\}dR' + RR'L'S_{12}(m_{12} - X')(m_{21} - X)dL \\
&+ R'(m_{12} - X')[RLS_{12}(m_{21} - X) - T(m_{11} - D)]dL' \\
&+ (R'(m_{12} - X')[R + (m_{11} - D)(M - L')] - \\
&- T'S_{12}[R + M(m_{11} - D)][R' + M'(m_{22} - D')])dT \\
&- TS_{12}[R + M(m_{11} - D)][R' + M'(m_{22} - D')]dT'\} / \\
&/\{T\,T'[R' + M'(m_{22} - D')][R + M(m_{11} - D)] \\
&- RR'LL'(m_{12} - X')(m_{21} - X)
\end{aligned}
\tag{2}
$$

dρ represents the uncertainty of reflection coefficient of any one-port DUT and it was given in [1], [2], while dS_{12} represents the differential error of S_{12} parameter of any two-port DUT, and it is given here for the first time. Notably, although these expressions are the more general ones, they are simplified a lot, when the SLO calibration standards are considered, and even more, when a direct Through connection is possible between the two ports.

Apparently from (1), three 3 system errors and one 1 unknown, the reflection coefficient of the DUT, are taking part in one-port measurements while the two-port measurements, from (2), include twelve 12 system errors and four 4 unknowns, the S-parameters of the DUT. Tab. 1 contains the analytical variable counting of all the involved quantities, complex and real. The total number of differentials and the specific type of the used calibration standards, will define the complexity of the final DER graphical construction.

Building a DER

As it is obvious from the expressions (1), (2) and Tab. 1, a great number of parameters are involved in the construction of a final actual DER. For simplicity it is as-

sumed that if z stands for any of independent parameter, either of a measurement or a Standard Load,

$$z = |z|e^{jy} \qquad (3)$$

then dz is its differential, that is, its inaccuracy or uncertainty respectively

$$dz = e^{jy}(d|z| + j|z|dy) \qquad (4)$$

Thus, if W is the known value of the respective partial derivative, e.g. of ρ or S

$$W = |W|e^{jV} \qquad (5)$$

then Wdz is a partial differential error

$$Wdz = e^{j(V + y)} \cdot$$
$$\cdot |W|(d|z| + j|z|dy) \qquad (6)$$

Each expression Wdz defines the contour of a partial z Differential Error Region on the complex plane around the origin O. Fig. 3 shows the six (6) steps needed for such a typical DER construction:

(1) d|z| as real and dy as imaginary part, are shown as vectors in the complex plane.

(2) dy is multiplied by |z| ≤ 1 thus their product will be, in general, less than dy. The figure contains all the possible values of these terms, plus or minus (±).

Tab. 1: Counting Variables

Response Calibration (Short)

   2 Measurements   → 2 Inaccuracies
   1 Standard Load   → 1 Uncertainty

   3 Complex Variables → 3 Complex Differential Errors

   6 Real Variables
   6 Real Differentials

Full One-Port Calibration

   4 Measurements   → 4 Inaccuracies
   3 Standard Loads   → 3 Uncertainties
   7 Complex Variables → 7 Complex Differential Errors

   14 Real Variables
   14 Real Differentials

Full Two-Port Calibration with Direct Through

  16 Measurements   → 16 Inaccuracies
   6 Standard Loads   → 6 Uncertainties
  22 Complex Variables → 22 Complex Differential Errors

   44 Real Variables
   44 Real Differentials

Full Two-Port Calibration with Indirect Through

  16 Measurements   → 16 Inaccuracies
   7 Standard Loads   → 10 Uncertainties (6+4)
  26 Complex Variables → 26 Complex Differential Errors

   52 Real Variables
   52 Real Differentials

(3) Four points in the complex plane result in after the vector addition.

(4) These four points forms the initial rectangular DER with the dotted line.

(5) This DER is either contracted/shrank or expanded/stretched as it is multiplied by the positive scaling factor |W|. In the figure it is expanded (dashed line).

(6) Finally, the scaled DER is rotated according to the argument of the e factor in Wdz expression [8].

Three basic figures of DERs within the unit circle are discriminated as they are depicted in Fig. 4:

(1) The orthogonal i-DER at any interior point of the unit circle given with the red color in Fig. 4.1.

(2) The half orthogonal c-DER for any contour point, as it is the case for the Open and Short Loads, with magenta color in Fig. 4.2. Special care must be taken not to exceed the unit circle, which means that the corresponding d|z| values are not symmetrical, and

(3) the circular o-DER at the origin O, with green color in Fig. 4.3, where the magnitude of z equals to 0 ($|z| = 0$) and its argument is indeterminate.

This is the case for the 50 [Ω] Load.

For the sake of the example completeness and without loss of generality, we made the assumption that the i-DER results from expansion while the c-DER from contraction (dashed line), of their initial rectangular DER (dotted line) after the appropriate rotation (solid line), as it is shown in Fig. 5.1 and 5.2 respectively.

The simplest and at the same time the most demonstrative example to construct a complex DER is to add the three types of Fig. 4 DERs. The main scope is to explain, step by step, the procedure of their graphical addition.

Fig. 6 contains all the needed steps. First, all the rectangular DERs must be added and at the end the circulars. Thus, in Fig. 6.1 the two rectangular regions are shown where the c-DER overlays the i-DER. The basic rule for their addition is the parallelogram rule. It has to be applied between the four (4) vertices of the red colored i-DER and each one vertex of the magenta colored c-DER. In other words c-DER is translated to the four i-DER vertices parallel to itself as shown in Fig. 6.2.

The outermost points in the complex plane that results from the addition of

the two regions shown in Fig. 6.3, form the new DER with the blue convex outline which has eight vertices in Fig. 6.4. It is obvious that if we continue to shift the c-DER to other points on the sides of the i-DER, then all the resulting points will lie inside this blue DER. This is the way of adding rectangular DERs. The addition of each one rectangular DER to the previous polygonal region will increase the number of vertices by four (4).

Next the circular o-DER must be added to this new blue polygonal region. In Fig. 6.5 the o-DER overlays the blue octagonal region. The o-DER must be shifted again to all the vertices of the octagonal region as it is shown in Fig. 6.6.

The determination of the outermost points of the new DER demands to find the perpendiculars to all line segments of the blue DER at its eight (8) vertices. In Fig. 6.7 they are drawn in black color and for two vertices they are indicated with the well known right angle, also in black color. The points of the new DER result from the intersection of these perpendiculars with the circle in each vertex. Thus, each circle contributes two (2) vertices, as shown in Fig. 6.8. The final DER has a contour of sixteen (16) vertices with eight (8) line segments and eight (8) circular arcs depicted in Fig. 6.9. The involved complex parameters are three (3) and we added two (2) rectangular DERs and one (1) circular DER.

It is obvious that the constructed DER in this example is not a symmetrical region since we added a non symmetrical partial c-DER. It is also a region in the complex plane. Therefore, if an estimation is needed either for the real and imaginary part, or for the magnitude and argument of ρ or S, (or of any other depended on them quantity) that is, for the black point inside the DER, the measured value, then the rectangular and polar uncertainties, respectively, must be determined. These are the differential error intervals, DEIs. In order to accomplish that, we have to find the circumscribed to the DER orthogonal and its projection on the coordinate axes, at the measurement point, as it is shown with red color in Fig. 6.10. The circumscribed annular sector to the DER at the measurement point with blue color in Fig. 6.11 among with its corresponding radials and arcs will derive the polar DEIs. Fig. 6.12 contains the final DER with its DEIs.
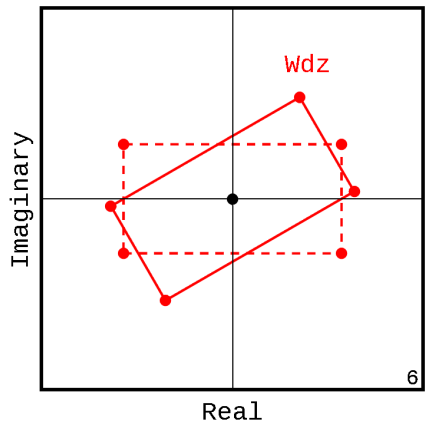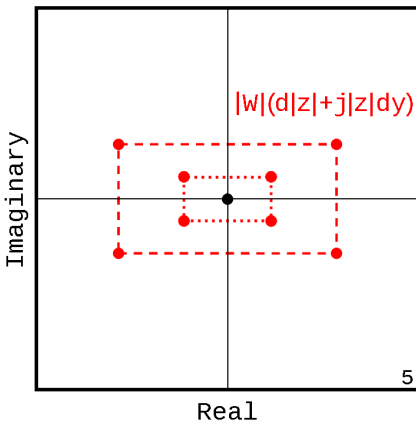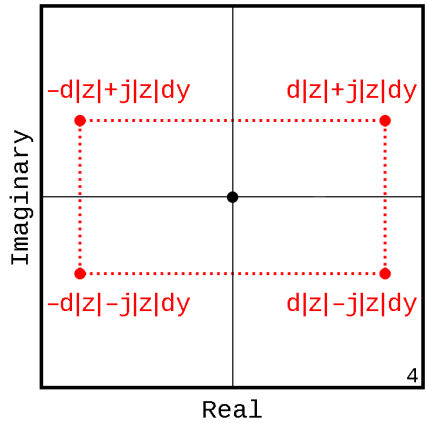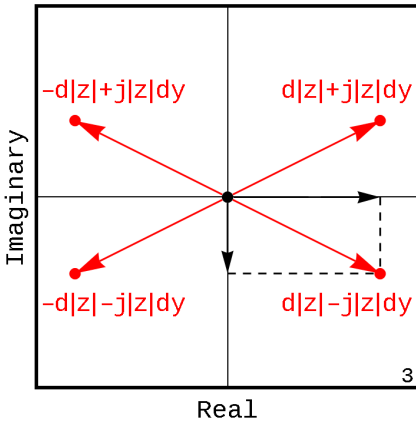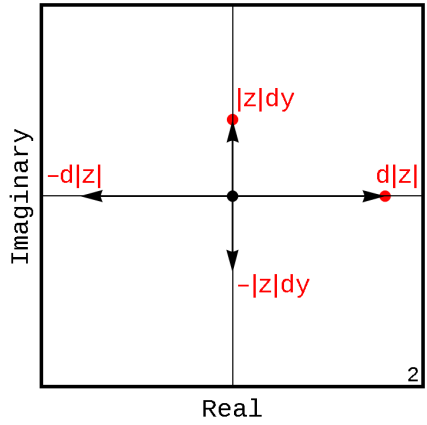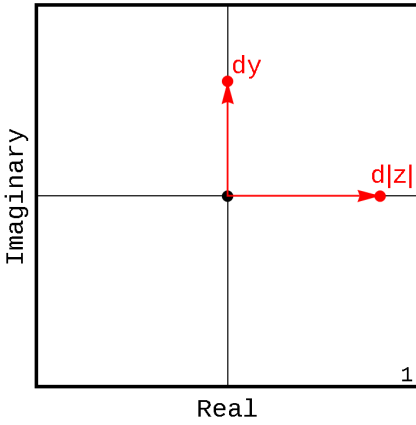
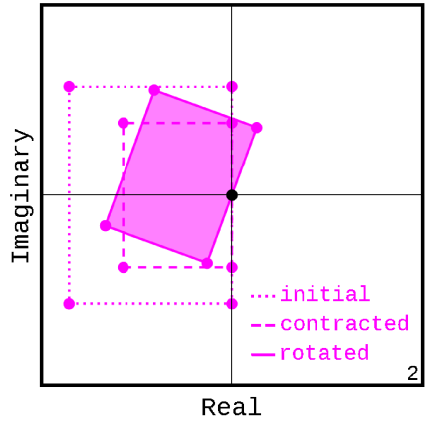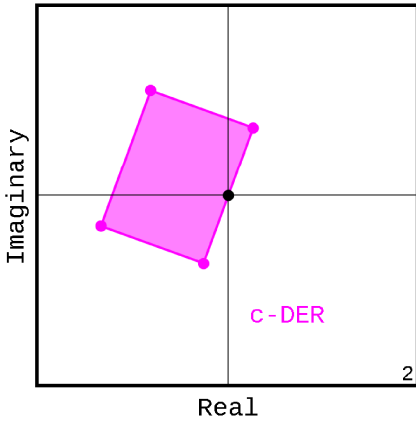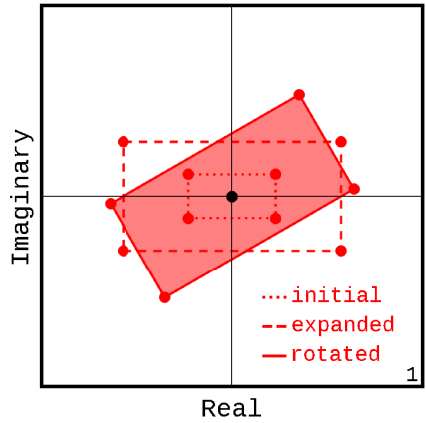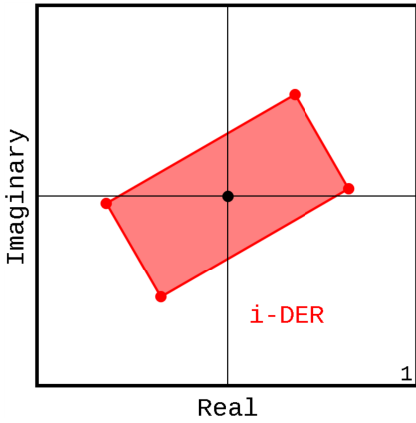Fig. 3.1-6: Wdz DER outline

Fig. 4.1-3: The 3 basic DERs
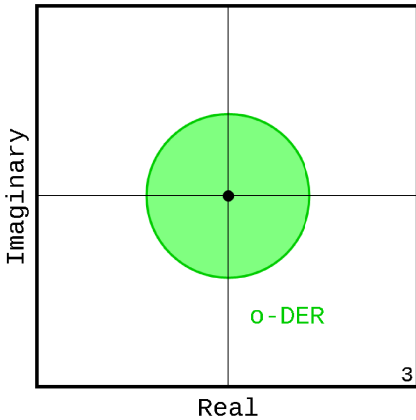
Fig. 5.1-2: Expanded, Contracted, and Rotated DERs

Application

Any complex DER is built from a number of basic DERs. Their number and type depend directly on the specific calibration technique applied on the measurements. Six appropriately selected DERs, of all those involved in the above measurements, are shown in Fig. 7 in order to demonstrate their great variety.
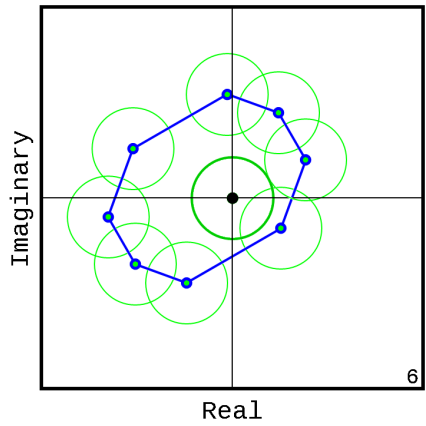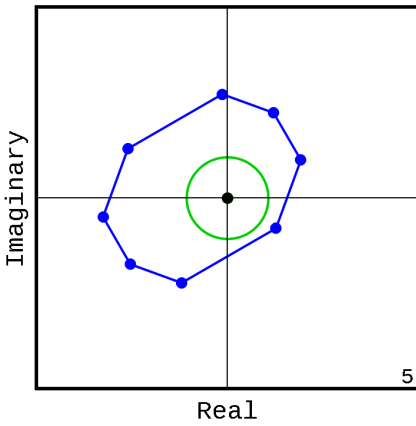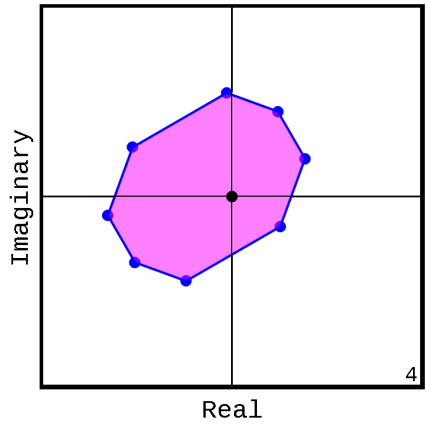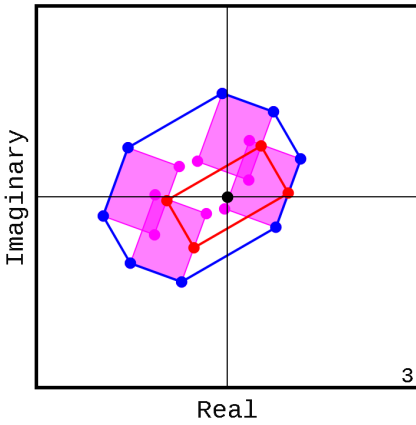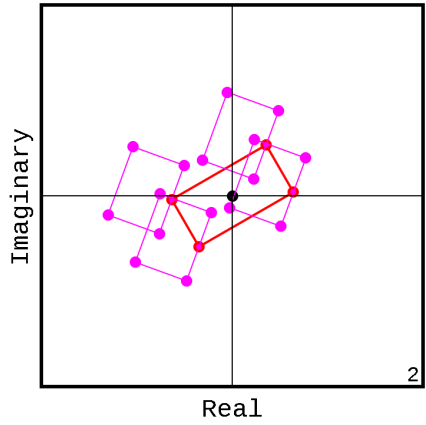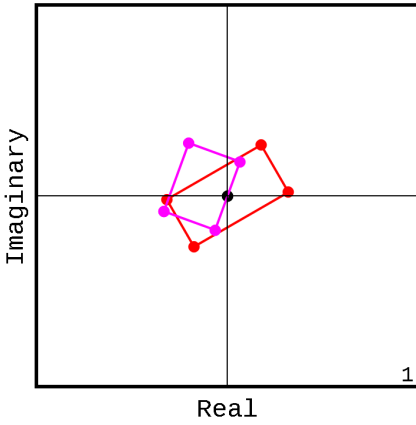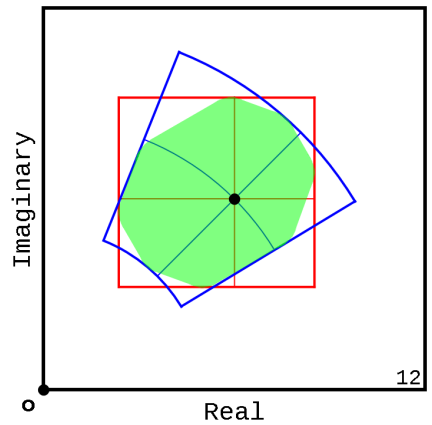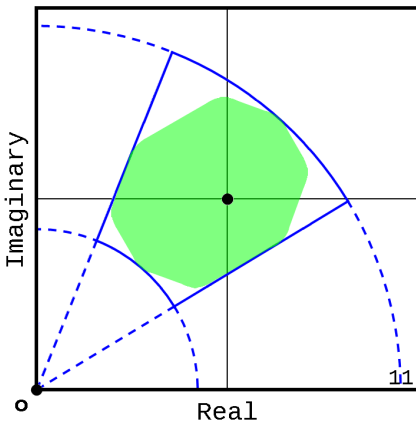
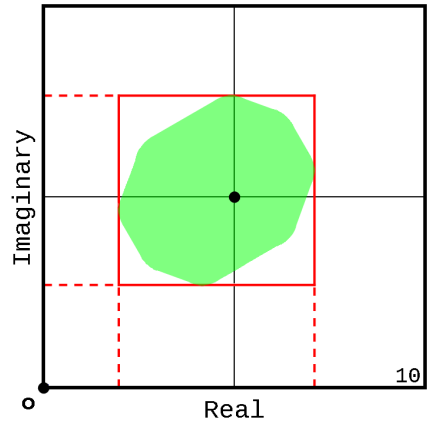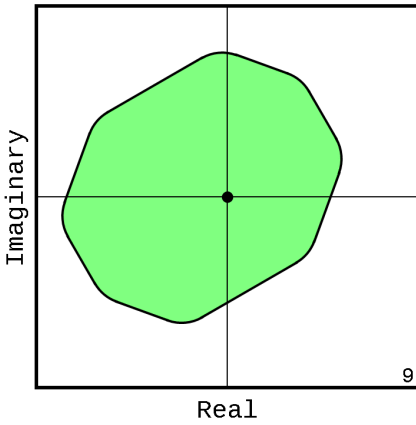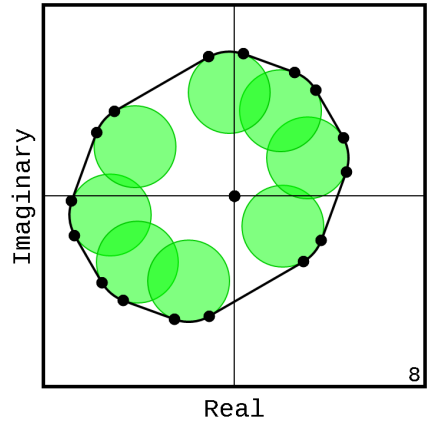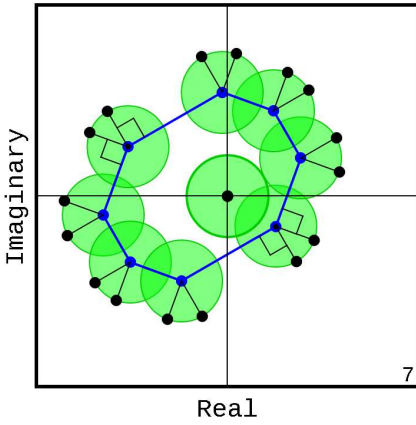Fig. 6a/b.1-6: Building a complex DER with its DEIs

Fig. 6b/b.7-12: Building a complex DER with its DEIs

Thus, the shape of DER: (a) in Fig. 7.1 and 7.4, is most influenced by its circular arcs, (b) in Fig.7.3, is almost near to a rectangle, while (c) in Fig. 7.6, the DER does not involve any o-DER.

Tab. 2 contains information for typical DERs with their number of vertices. For example, if the SLO standards are used for a one-port calibration then a ρ-DER is the sum of six (6) rectangles and one (1) circle and will have 6 x 4 = 24, 24 x 2 = 48 vertices at most while after a SLOdT calibration the vertices of an S-DER will be 20 x 4 = 80, 80 x 2 = 160 at most.

A few representative applications are shown in Figs.

8-12 from already published author's work. Fig. 8 shows the antenna input impedance, resistance and reactance, for a ground plane antenna with the dashed line from simulation [1], [6]. In Fig. 9 the Standing Wave Ratio of a radial discone antenna with 60° cone apex is illustrated with the solid line from simulation as in [2] but only in the measured frequency range. Fig. 10 shows the S-matrix of a two antennas system at one frequency with the one antenna to be rotated [3]. Fig. 11 shows the Z-matrix of a T-network [3], [4] and Fig. 12 contains the antenna patterns for amplitude and phase with the dashed line from simulation [3].

Tab. 2: Number of DER's vertices

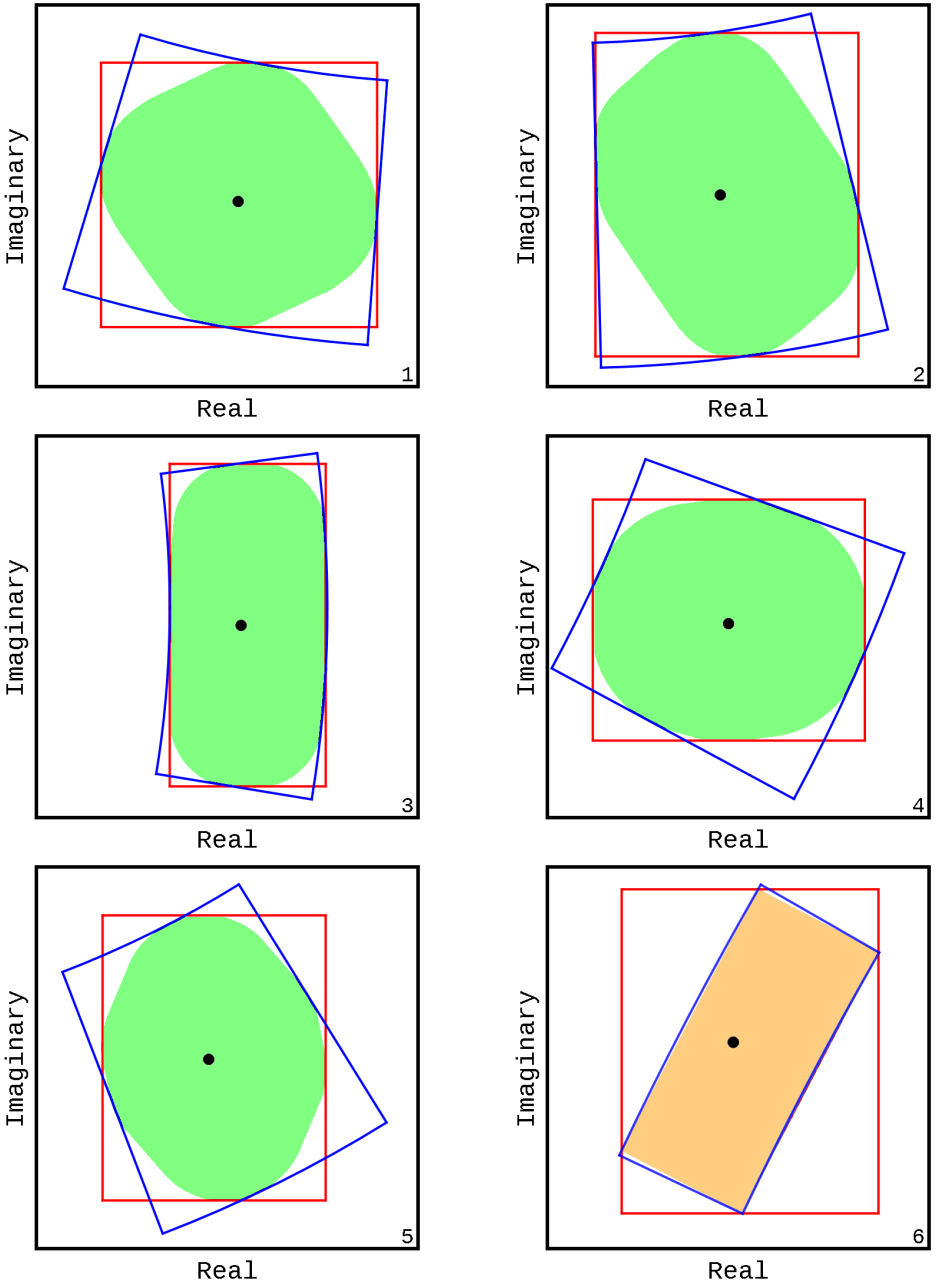| General Calibration			
ρ-DER	7 Rectangles x 4 vertices	28 vertices	
S-DER	22 Rectangles x 4 vertices	88 vertices	
Response Calibration			
ρ-DER	3 Rectangles x 4 vertices	12 vertices	[6]
SLO/SLOdT/SLOT Calibration			
ρ-DER SLO	6 Rectangles + 1 Circles	48 vertices	[1],[2]
S-DER SLOdT	20 Rectangles + 2 Circles	160 vertices	[3],[4]
S-DER SLOT	22 Rectangles + 4 Circles	176 Vertices	[5]

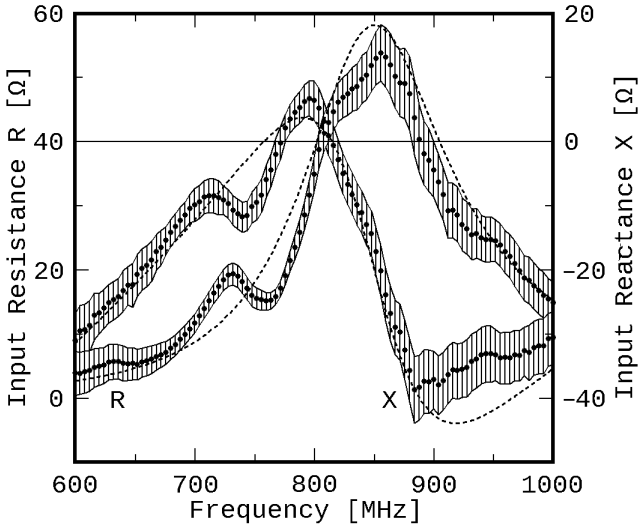Fig. 7.1-6: Six actual complex DERs of various shapes

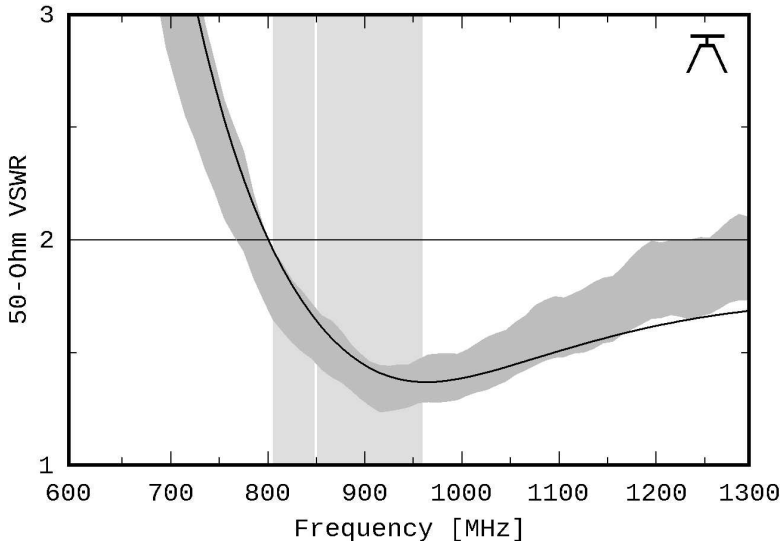Fig. 8: Rectangular DEIs of input impedance
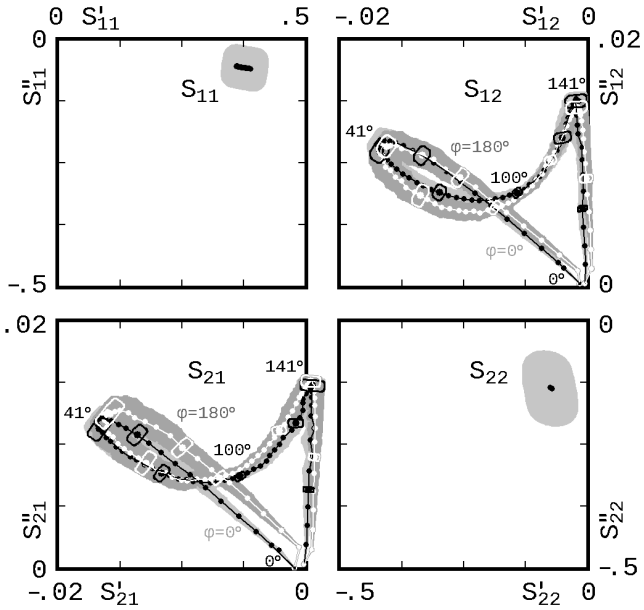

Fig. 9: DEIs of a discone antenna Standing Wave Ration
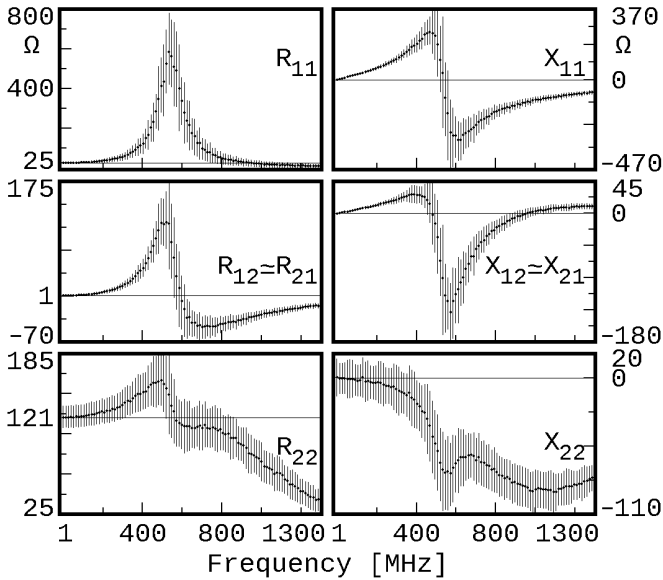
Fig. 10: S-Matrix of a two antennas system
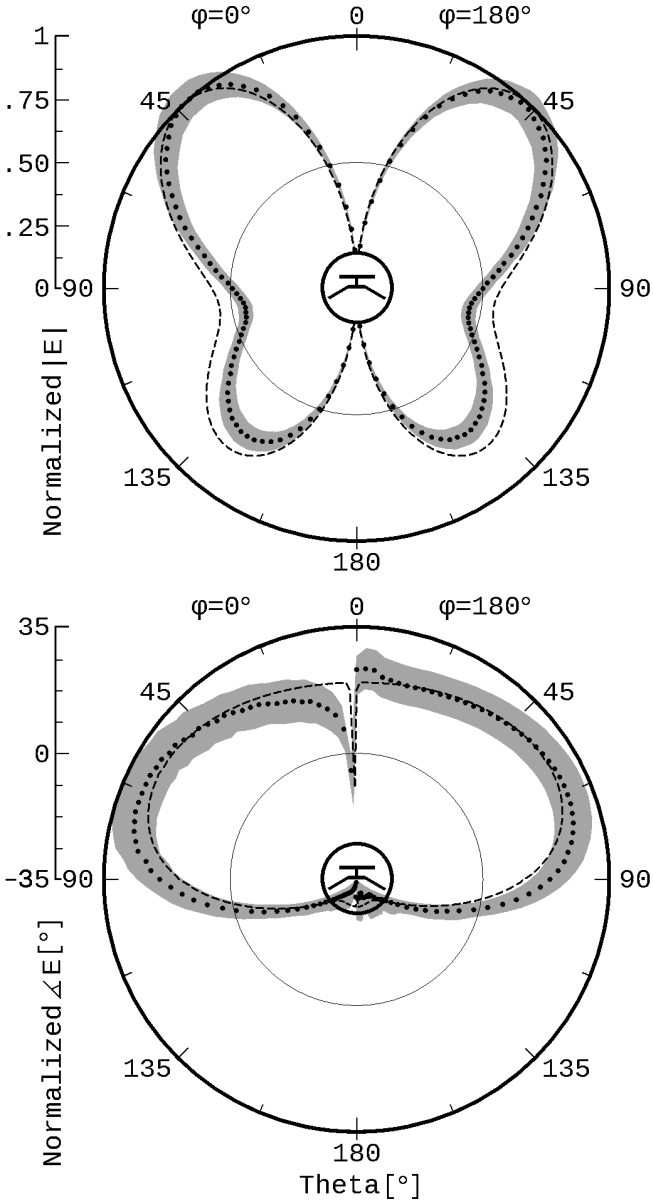

Fig. 11: Z-DEIs against frequency

Fig. 12: Antenna amplitude and phase patterns

Conclusion

The geometric representation of complex DERs and real DEIs, as well as, the graphical construction of them were presented, as the fifth part of this series of papers, for one- and two-port VNA measurement uncertainties. The adopted step-by-step procedure illustrates the following remarks:

1. It is not possible to analytically express an estimation for a real existing uncertainty of the real and imaginary parts of a complex VNA measurement: first, by considering them as real functions of complex variables, of any Error Model, and then, by attempting to differentiate them, because every partial derivative of a non-constant real function of a complex variable does not exist.

2. However, it is possible to analytically estimate real uncertainties from the graphically constructed DER in the complex plane.

2.(a): The two real rectangular uncertainties, that is the uncertainty of real and imaginary part of the complex measurement, can be computed from the corresponding two sides of the unique orthogonal parallelogram circumscribed to DER, which we introduced as the concept of Real Rectangular DEIs, e.g. Fig.6b/b.10. And these uncertainties are estimable because the two end-points of each rectangular DEI are expressed by sharp inequalities.

2.(b): The two real polar uncertainties, that is the uncertainty in magnitude and argument of the complex measurement, can be determined from the corresponding arcs and radials of the unique annular sector circumscribed to DER, which we introduced as the concept of Real Polar DEIs, e.g. Fig.6b/b.11. And these uncertainties are estimable because the two end-points of each polar DEI are algorithmically expressed by sharp inequalities.

3. Notably, the proposed method of uncertainty estimation, with the construction of complex DERs, can be applied to any VNA calibration technique, because it is valid for any number of considered parameters.

4. Finally, we have to emphasize that this technique of uncertainty estimation does not predict the final shape of a DER in advance, because a rather complicated algorithm is needed for that instead.

In a next part of this series of papers, we will present, in details, the implementation of this invented technique with developed computer FLOSS applications in order to produce and cross check the results needed to construct any DERs and DEIs, using: the Open Watcom FORTRAN FLOSS, BBCBasic Demo, Maxima FLOSS, and Mathematica.

References

[1] Yannopoulou N., Zimourtopoulos P., "Total Differential Errors in One Port Network Analyzer Measurements with Application to Antenna Impedance", Radioengineering, Vol. 16, No. 2, June 2007, pp. 1 - 8
www.radioeng.cz/fulltexts/2007/07_02_01_08.pdf

[2] Yannopoulou N.I., Zimourtopoulos P.E., "Measurement Uncertainty in Network Analyzers: Differential Error Analysis of Error Models Part 1: Full One-Port Calibration", FunkTechnikPlus # Journal, Issue 1, Year 1, October 2013, pp.17 - 22
www.otoiser.org/index.php/ftpj/article/view/42/37

[3] Yannopoulou N., Zimourtopoulos P., "S-Parameter Uncertainties in Network Analyzer Measurements with Application to Antenna Patterns" Radioengineering, Vol. 17, No. 1, April 2008,pp. 1 - 8
www.radioeng.cz/fulltexts/2008/08_01_01_08.pdf

[4] Yannopoulou N.I., Zimourtopoulos P.I., "Measurement Uncertainty in Network Analyzers: Differential Error Analysis of Error Models Part 2: Full Two-Port Calibration", FunkTechnikPlus # Journal, Issue 1, Year 1, 2013, pp. 23 - 30 www.otoiser.org/index.php/ftpj/article/view/43/38

[5] Yannopoulou N.I., Zimourtopoulos P.I., "Measurement Uncertainty in Network Analyzers: Differential Error Analysis of Error Models Part 4: Non-Zero Length Through in Full Two-Port SLOT Calibration", FunkTechnikPlus # Journal, Issue 11, Year 4, 2016, pp. 7 - 29
www.otoiser.org/index.php/ftpj/article/view/60/53

[6] Yannopoulou N.I., Zimourtopoulos P.I., "Measurement Un-
    certainty in Network Analyzers: Differential Error Anal-
    ysis of Error Models Part 3: Short One-Port Calibration
    – Comparison", FunkTechnikPlus # Journal, Issue 2, Year
    1, 2013, pp. 41 - 49
    www.otoiser.org/index.php/ftpj/article/view/44/39
[7] Yannopoulou N.I., Zimourtopoulos P.I., "Building Complex
    Differential Error Regions",
    "http://resource.npl.co.uk/docs/networks/anamet/members_
    only/meetings/30/yannopoulou_zimourtopoulos.pdf",
    www.antennas.gr/anamet/30/
[8] Bonfert-Taylor P., "Introduction to Complex Analysis",
    "Analysis of a Complex Kind", Online Coursera Course,
    Summer 2016, Week 4, Lecture 3, "Möbius transformations"
    www.coursera.org/learn/complex-analysis
    *Active Links: 25.05.2018 - Inactive Links : FTP#J Link
    Updates: http://updates.ftpj.otoiser.org/

* About The Authors

Nikolitsa Yannopoulou, Issue 9, Year 3, p. 390

yin@arg.op4.eu

Petros Zimourtopoulos, Issue 9, Year 3, p. 390

pez@arg.op4.eu